

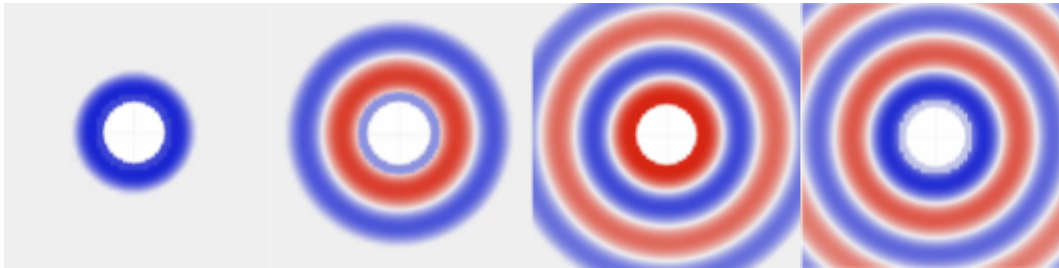


Gecko

Design for IGA-type  
discretization workflows

## Gecko Technical Report 2

### DC8 – Dođuhan Kılıçarslan



This project has received funding from the European Union's Horizon Europe research and innovation programme under grant agreement No 101073106  
Call: HORIZON-MSCA-2021-DN-01

Funded by the  
European Union

#### Executive summary

---

This technical report is comprised of the research conducted about transient acoustics with the implementation and verification of the time domain boundary element method alongside the solution acceleration methods to reduce the storage and computational requirements. Moreover, future plans to progress in the research is included.



## Table of contents

---

Executive summary	2
Table of contents	3
List of figures	4
List of tables	4
List of abbreviations	5
Introduction	6
1. Transient Acoustic BEM	7
1.1. Theory	7
1.2. Implementation & Results	7
2. Accelerated Solution Methodologies	8
2.1. Theory	8
2.2. Numerical Examples	9
3. Conclusion	11
4. References	12

## List of figures

---

Figure 1: *Numerical results compared with analytical result for chosen points in rectangular (a) and circular (b) geometry.* 8

Figure 2: *Example geometries and their sampling points for internal excitation (a), harmonic external excitation (b), and plane wave excitation (c).* 10

Figure 3: *Truncation error against the changing  $\delta$ -parameter for different orders of expansion for the problems given in Fig. 2 (a), (b), and (c), respectively.* 10

## List of tables

---

Table 1: *Obtained reductions for different orders of expansion and different problems* 11

## List of abbreviations

---

<i>IGA</i>	<i>IsoGeometric Analysis</i>
<i>FEM</i>	<i>Finite Element Method</i>
<i>FEA</i>	<i>Finite Element Analysis</i>
<i>CAD</i>	<i>Computer Aided Design</i>
<i>NURBS</i>	<i>Non-Uniform Rational B-Splines</i>
<i>BEM</i>	<i>Boundary Element Method</i>
<i>MOR</i>	<i>Model Order Reduction</i>

## Introduction

---

Even though acoustics is mostly related with frequency domain problems and solution techniques there are still many problems that require transient solutions, such as; Auralization problem where the time of arrival of a sound to both ears are different and transient solution is required to understand the human hearing [1], or, pass-by-noise problem [2] where the moving cars creates traffic noises which generally requires transient modelling of the problem. There are also problems that the input signal is directly generated by transient sound sources that carry frequency signals changing in time such as engine run-up noise [3]. Computational requirements are exceptionally high because these simulations rely on time-domain analyses and/or convolution calculations, coupled with the fine meshes needed to capture the intricate geometric details. On top of that, many of the aforementioned problems require remeshing due to changing conditions or to take care of the uncertainties which increases the computational burden for the simulation further. Where the computational cost and accuracy errors reach a critical threshold, even experimental testing may become a more viable alternative than numerical simulations.

Isogeometric Analysis (IGA), proposed by Hughes et. al. [4], tries to combine computer aided design (CAD) with finite element analysis (FEA), and, while doing so offers a robust solution to combination of problems mentioned. By utilizing CAD geometry descriptions, such as non-uniform rational B-splines (NURBS), as FEA shape functions, geometry is exactly represented which eliminates any discretization error and reduces the “fineness” of the mesh such that the original size of the system is reduced without losing details. Moreover, since the changes in the geometry is reflected directly to FEA description, need for meshing (ergo remeshing) is eliminated. Specially for time domain analysis, IGA also enables the use of similarly sized elements without losing the geometric details or using many elements with less detailed regions just to increase or preserve the stability of the problem. Finally, since NURBS has great flexibility with relatively low number of parameters it is also very efficient for topology optimization problems [5] that is placed in between CAD and FEA such that IGA is very beneficial to bridge that gap as well [6]

However, as many solutions in engineering IGA also comes with some new or exasperated older problems. One such problem is that finite element method (FEM) requires volume meshes in 3 dimensions and surface meshes in 2 dimensions while CAD representations are generally surfaces and lines for 3 and 2 dimensions, respectively. Hence, special methods may become necessary to apply IGA efficiently to complex and trimmed geometries such cutFEM [7], isogeometric boundary representation analysis [8], or shifted boundary method [9]. Alternative is to not use FEM, but instead to use boundary element method (BEM) in which only boundary is required such that it matches with CAD representations [10] even though it comes with its own problems such as non-conforming patches present in general CAD drawings [11].

In this report application of IGA workflows to transient acoustic problems are investigated, and their implementations, and accelerated solution methods are shown.

# 1. Transient acoustics BEM

## 1.1 Theory

Governing differential equation for transient acoustics is known as acoustic wave equation and is written as,

$$c^2 \nabla^2 p(r, t) - \frac{1}{c^2} \frac{\partial^2 p(r, t)}{\partial t^2} = f(r, t), \quad \text{in } \Omega$$

where  $p$  is the pressure,  $c$  is the speed of sound,  $f$  is a general acoustic excitation. Here  $\nabla^2$  is the Laplacian operator defined as  $\nabla^2 = \frac{\partial^2}{\partial x^2} + \frac{\partial^2}{\partial y^2} + \frac{\partial^2}{\partial z^2}$  in cartesian coordinates.

BEM starts by defining a representation formula in which function values inside the domain  $\Omega$  can be represented from the function values on the boundary  $\Gamma$  of the same domain [12]. For a static case without the excitation (for simplicity), equation can be written as,

$$p(r) = \int_{\Gamma} (p^*(\xi, r)(\nabla p(\xi) \cdot n) - (\nabla p^*(\xi, r) \cdot n)p(\xi)) d\Gamma,$$

where  $p^*$  is the fundamental solution that is defined by the response of a point source in an infinite domain, and  $n$  is the normal vector pointing out of the domain for the given boundary. If  $r$  is chosen to be on the boundary in a limiting process, same equation can be used to solve for the unknown boundary values of the function.

For the time domain analysis same logic applies with a change of time response of an impulsive point source applied in an infinite domain and an additional time integral given as,

$$p(\xi, t) = \int_0^t \int_{\Gamma} (p^*(\xi, \tau, r, t)(\nabla p(\xi, \tau) \cdot n) - (\nabla p^*(\xi, \tau, r, t) \cdot n)p(\xi, \tau)) d\Gamma d\tau.$$

When  $r$  is chosen to be on the boundary with a limiting process in space and time, and functions are discretized on the boundary [13], equation of motion in the matrix form is constructed as,

$$H_{nm} p_n - G_{nn} q_n = \sum_{m=1}^{n-1} (G_{nm} q_m - H_{nm} p_m) + f_n, \quad n = 1, 2, 3, \dots, N_t$$

where the index  $n$  refers to the  $n^{\text{th}}$  discrete time step,  $N_t$  is the total number of time steps, and the summation term is due to the convolution nature of the representation formula. Solution for the unknowns at time step  $n$  can be obtained by first obtaining the solution for the earlier time steps  $m$  starting from the initial time. This time marching procedure can be quite expensive to calculate and store.

## 1.2 Implementation & Results

In the first report [14] a 2D Time Domain BEM (TD-BEM) code was developed using linear shape functions and was verified with the analytical solutions. Sample verification graphs are given in Fig. (1) for a step response in a rectangular geometry, and, harmonically excited external domain by a circular geometry.

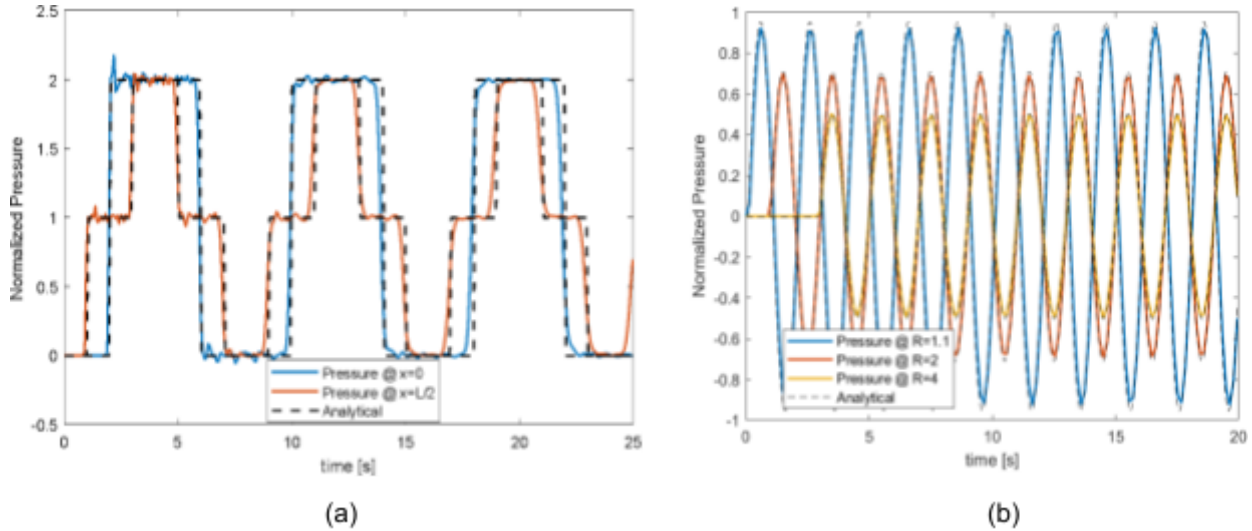


**Figure 1:** Numerical results compared with analytical result for chosen points in rectangular (a) and circular (b) geometry.

## 2. Accelerated Solution Methodologies

### 2.1 Theory

Solution method of TD-BEM, as presented in [14], requires time marching, which has the asymptotic scaling for storage on the order of  $\sim O(N_t N_s^2)$ , and for computation on the order of  $\sim O(N_t^2 N_s^2)$ , where  $N_s$  is the total spatial degrees of freedom. Resulting in excessive storage requirements as well as computational load for longer time simulations, making the method unfeasible for practical applications. In this chapter, a novel method for the acceleration of solution is developed which enables TD-BEM to be applied to longer-duration simulations.

Initial direction is set by a simple idea of truncating the summation of past terms after some time has passed [15], shown mathematically as,

$$H_{nm} p_n - G_{nm} q_n = \sum_{m=(n-N_L, 1)}^{n-1} (G_{nm} q_m - H_{nm} p_m) + f_n, \quad n = 1, 2, 3, \dots, N_t.$$

Resulting formula directly disregards contributions coming from earlier than  $N_L$  number of time steps past from the summation, which reduces the calculations and storage and does not cause significant problems for exterior problems with low number of reflections. However, if the problem has a lot of reflections and/or it is interior, truncation can introduce significant error and

can even make the solution unstable [16]. To control this truncation error  $\delta$  parameter is introduced which corresponds to ratio of the lost information if  $p^*$  is truncated after some time at the average distance of the geometry. Defined mathematically as,

$$\delta = \frac{\int_0^{t-t_L} p^* d\tau}{\int_0^{t-r_{avg}} p^* d\tau},$$

for which it could be solved analytically to obtain truncation limit time  $t_L = N_L \Delta t$  for a given  $\delta$ . Even though it is not a error predictor it can be used to control and limit the error.

Next step in the development is to add a correction terms to reduce the truncation error while introducing smaller number of matrices. Since the analytical form for the fundamental solution is available, Taylor Series Expansion is used separate the temporal and spatial variables [16]. Resulting expanded fundamental solution in 2D can be written as,

$$p^* = \frac{2c}{\sqrt{c^2 \Delta t^2 - r^2}} \hat{H}(c\Delta t - r) \cong \frac{2c}{(c^2 \Delta t^2 - r_{rep}^2)^{\frac{1}{2}}} + \frac{2cr_{rep}(r-r_{rep})}{(c^2 \Delta t^2 - r_{rep}^2)^{\frac{3}{2}}} + \dots,$$

where  $\Delta t$  is the time separation of the source and the observer while  $r$  is the space separation, and  $r_{rep}$  is the representative distance the expansion takes place and is generally taken to be the average distance in the geometry. Using the expanded form in the integral calculations of TD-BEM produces system matrices depending only on the distance and the expansion order, and separate temporal scalar functions that depend on the time and the expansion order. Resulting truncated equation of motion after the truncation limit can be written as,

$$H_{nn} p_n - G_{nm} q_n = \sum_{m=n-N_L}^{n-1} (G_{nm} q_m - H_{nm} p_m) + \sum_{m=1}^{n-N_L-1} (G_{nm}^* q_m - H_{nm}^* p_m) + f_n.$$

Here the reduced matrices are constructed from the expansion orders as,

$$G^* = \sum_{k=1}^{N_o} G^k \left( (r - r_{rep})^k \right) * g_{nm}(\Delta t), \quad H^* = \sum_{k=1}^{N_o} H^k \left( \frac{\partial r}{\partial n} (r - r_{rep})^k \right) * h_{nm}(\Delta t),$$

where  $N_o$  is the number of terms included in the expansion,  $G^k$  and  $H^k$  are static matrices that depend on their argument and  $g_{nm}$  and  $h_{nm}$  are scalar function depending on time separation. Exact analytical form for both of them exists but is not given here for brevity.

Resulting equation achieves  $\sim O((N_o + N_L)N_s^2)$  scaling for storage and  $\sim O((N_o + N_L)N_t N_s^2)$  for matrix computation. Assuming  $N_L$  can be reduced independent of  $N_t$  with increasing  $N_o$ , both scaling lows reduce one order of dependency to number of time steps. In practice this is achieved since  $N_L$  depends on the size of the geometry rather than total time simulation, which will be examined in the next section.

## 2.2 Numerical Examples

Geometries available in the first report [14] and a new complex shape is used in the analysis for which series truncated solutions are compared with the full solutions. Maximum error obtained for the whole simulation are combined for three points, mathematically described as,

$$\epsilon_{L_2} = \sqrt{\sum_{i=1}^3 \left( p_i^{full}(t) - p_i^{series}(t) \right)^2}.$$

Problems include a step boundary excitation in a rectangular geometry for interior domain, harmonically excited boundary on circular geometry for exterior domain, and single sine plane wave excitation with a disproportionate geometry for exterior domain, as given in Fig. 2. Resulting truncation error is also graphed in Fig. 3 for different orders of expansion and changing  $\delta$ -parameter.

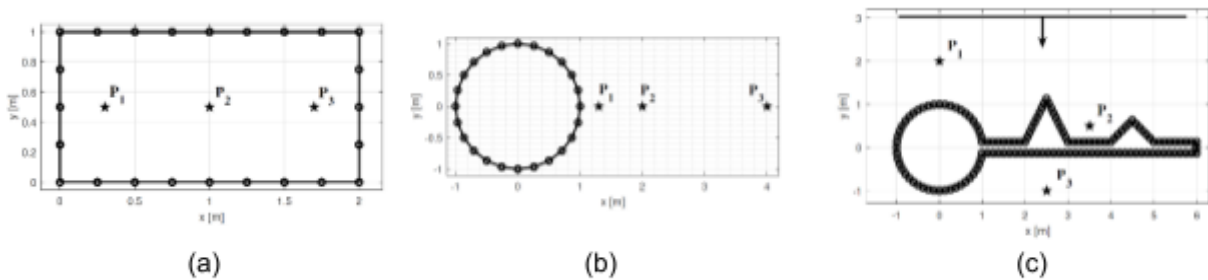
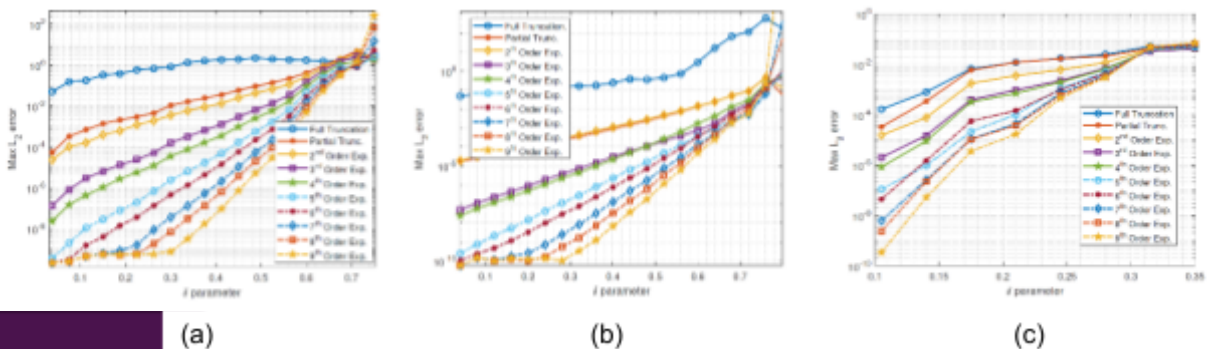


**Figure 2:** Example geometries and their sampling points for internal excitation (a), harmonic external excitation (b), and plane wave excitation (c).

As can be seen for all examples the trend is the same in which increasing the order of expansion produces lower error up to the numerical precision of the problem, which corresponds to low to moderate reductions can be achieved without introducing error. Moreover, significant reductions can be achieved depending on the error tolerance of the problem.

Second thing to note is that nearly all of the orders of truncation converge around a similar error for a similar  $\delta$  value, which corresponds to the causality limit of the problem. If the truncation starts before the fundamental solution of each point on the geometry has time to reach all points of the geometry, pressure arrives to those points before intended which causes instabilities in the solution. This is the limiting factor for the choice of  $N_L$ , after which increasing  $N_o$  does not decrease the error but increase it. Since, this causality limit only depend on the maximum



distance of the geometry and the speed of sound  $N_L$  can be picked separately to  $N_t$ . While it does not guarantee  $N_o$  is separate from  $N_t$ , in practice it is observed to be.

**Figure 3:** Truncation error against the changing  $\delta$ -parameter for different orders of expansion for the problems given in Fig. 2 (a), (b), and (c), respectively.

Finally, to observe the reduction rate for a given expansion order an error criteria needs to be defined to select  $\delta$ -parameter accordingly. By choosing an error criteria of 0.1% Table 1 can be constructed which shows the reduction obtained  $((N_t - N_o - N_L)/N_t)$  for selected orders of expansion. Significant reductions can be achieved with some diminishing returns with increased orders, for the problems analysed, 5<sup>th</sup> order expansion seems to be the most logical choice but each problem has separate optimum value, which may depend on other factors such as total simulation time,  $r_{rep}$  choice, as well as the shape of the geometry. Considering error rates are also calculated after the full solution, a more comprehensive a priori error estimate that depends on the aforementioned parameters need to be developed to make the method more viable.

Problem	Order of expansion					
	None	1 <sup>st</sup>	2 <sup>nd</sup>	3 <sup>rd</sup>	5 <sup>th</sup>	9 <sup>th</sup>
(a)	0%	38%	55%	76%	82%	83%
(b)	0%	75%	67%	87%	86%	84%
(c)	30%	30%	49%	50%	51%	52%

**Table 1:** Obtained reductions for different orders of expansion and different problems

### 3. CONCLUSIONS

In this report transient acoustic analysis is researched and investigated for in BEM context with explicit time integration using convolution type methods. Furthermore TD-BEM implementation is accelerated through the use of truncation and series expansions. Advantages of applying acceleration techniques is highlighted and examples supporting it are given. Finally need for an a priori error estimate is emphasised. In the future IGA and MOR methods will be applied on the already developed tools to obtain novel results.

## 4. REFERENCES

- [1] M. Vorländer, *Auralization: Fundamentals of Acoustics, Modelling, Simulation, Algorithms and Acoustic Virtual Reality*. in RWTHedition. Cham: Springer International Publishing, 2020. doi: 10.1007/978-3-030-51202-6.
- [2] J. Morel, C. Marquis-Favre, and L.-A. Gille, “Noise annoyance assessment of various urban road vehicle pass-by noises in isolation and combined with industrial noise: A laboratory study,” *Applied Acoustics*, vol. 101, pp. 47-57, Jan. 2016, doi: 10.1016/j.apacoust.2015.07.0`.
- [3] J.-G. Ih, H.-J. Kim, S.-H. Lee, and K. Shinoda, “Prediction of intake noise of an automotive engine in run-up condition,” *Applied Acoustics*, vol. 70, no. 2, pp. 347-355, Feb. 2009, doi: 10.1016/j.apacoust.2008.03.007.
- [4] T. J. R. Hughes, J. A. Cottrell, and Y. Bazilevs, “Isogeometric analysis: CAD, finite elements, NURBS, exact geometry and mesh refinement,” *Computer Methods in Applied Mechanics and Engineering*, vol. 194, no. 39-41, pp. 4135-4195, Oct. 2005, doi: 10.1016/j.cma.2004.10.008.
- [5] T. Takahashi, N. Miyazawa, and M. Tanigawa, “A three-dimensional shape optimization for transient acoustic scattering problems using the time-domain boundary element method,” *Numerical Meth Engineering*, vol. 124, no. 2, pp. 482-512, Jan. 2023, doi: 10.1002/nme.7130.
- [6] Y. Wang, Z. Wang, Z. Xia, and L. Hien Poh, “Structural Design Optimization Using Isogeometric Analysis: A Comprehensive Review,” *CMES*, vol. 117, no. 3, pp. 455-507, Dec. 2018, doi: 10.31614/cmcs.2018.04603.
- [7] V. P. Nguyen, C. Anitescu, S. P. A. Bordas, and T. Rabczuk, “Isogeometric analysis: An overview and computer implementation aspects,” *Mathematics and Computers in Simulation*, vol. 117, pp. 89-116, Nov. 2015, doi: 10.1016/j.matcom.2015.05.008.
- [8] M. Breitenberger, A. Apostolatos, B. Philipp, R. Wüchner, and K.-U. Bletzinger, “Analysis in computer aided design: Nonlinear isogeometric B-Rep analysis of shell structures,” *Computer Methods in Applied Mechanics and Engineering*, vol. 284, pp. 401-457, Feb. 2015, doi: 10.1016/j.cma.2014.09.033.
- [9] N. Antonelli *et al.*, “The Shifted Boundary Method in Isogeometric Analysis,” *Computer Methods in Applied Mechanics and Engineering*, vol. 430, p. 117228, Oct. 2024, doi: 10.1016/j.cma.2024.117228.
- [10] R. N. Simpson, M. A. Scott, M. Taus, D. C. Thomas, and H. Lian, “Acoustic isogeometric boundary element analysis,” *Computer Methods in Applied Mechanics and Engineering*, vol. 269, pp. 265-290, Feb. 2014, doi: 10.1016/j.cma.2013.10.026.
- [11] L. Coox, F. Greco, O. Atak, D. Vandepitte, and W. Desmet, “A robust patch coupling method for NURBS-based isogeometric analysis of non-conforming

multipatch surfaces,” *Computer Methods in Applied Mechanics and Engineering*, vol. 316, pp. 235-260, Apr. 2017, doi: 10.1016/j.cma.2016.06.022.

[12] L. Gaul, M. Kögl, and M. Wagner, *Boundary Element Methods for Engineers and Scientists*. Berlin, Heidelberg: Springer Berlin Heidelberg, 2003. doi: 10.1007/978-3-662-05136-8.

[13] J. Dominguez, *Boundary elements in dynamics*. in International series on computational engineering. Southampton Boston London New York: Computational mechanics publ. Elsevier applied science, 1993.

[14] D. Kılıçarslan, GECKO DC Technical Reports 1 (Feb 2025). Retrieved from website:  
[https://gecko.cimne.com/wp-content/uploads/sites/4/2025/02/DC8\\_Technical\\_Report.pdf](https://gecko.cimne.com/wp-content/uploads/sites/4/2025/02/DC8_Technical_Report.pdf)

[15] V. Demirel and S. Wang, “An efficient boundary element method for two-dimensional transient wave propagation problems,” *Applied Mathematical Modelling*, vol. 11, no. 6, pp. 411-416, Dec. 1987, doi: 10.1016/0307-904X(87)90165-X.

[16] D. Kılıçarslan, D. Panagiotopoulos, and E. Deckers, “Investigation of Memory Efficient Convolutional Truncation Methods for the 2D Time Domain Boundary Element Method,” in *Proceedings of the 11th Convention of the European Acoustics Association Forum Acusticum / EuroNoise 2025*, Málaga, Spain: European Acoustics Association, Dec. 2025, pp. 5351-5358. doi: 10.61782/fa.2025.0503.